High-accuracy mass measurements of neutron-rich Kr isotopes

P. Delahaye,[1] G. Audi,[2] K. Blaum,[3,4] F. Carrel,[4,*] S. George,[3,4] F. Herfurth,[4] A. Herlert,[5,†] A. Kellerbauer,[1,‡]
H.-J. Kluge,[4,6] D. Lunney,[2] L. Schweikhard,[5] and C. Yazidjian[4]

[1]*ISOLDE, CERN, Physics Department, CH-1211 Geneva 23, Switzerland*
[2]*CSNSM-CNRS-IN2P3, F-91405 Orsay, France*
[3]*Johannes Gutenberg-Universität, Institut für Physik, D-55099 Mainz, Germany*
[4]*Gesellschaft für Schwerionenforschung GSI, D-64291 Darmstadt, Germany*
[5]*Ernst-Moritz-Arndt-Universität, Institut für Physik, D-17487 Greifswald, Germany*
[6]*Ruprecht-Karls-Universität Heidelberg, Physikalisches Institut, D-69120 Heidelberg, Germany*

The atomic masses of the neutron-rich krypton isotopes $^{84,86-95}$Kr have been determined with the tandem Penning trap mass spectrometer ISOLTRAP with uncertainties ranging from 20 to 220 ppb. The masses of the short-lived isotopes ^{94}Kr and ^{95}Kr were measured for the first time. The masses of the radioactive nuclides ^{89}Kr and ^{91}Kr disagree by 4 and 6 standard deviations, respectively, from the present Atomic-Mass Evaluation database. The resulting modification of the mass surface with respect to the two-neutron separation energies as well as implications for mass models and stellar nucleosynthesis are discussed.

I. INTRODUCTION

As a measure of the total nuclear binding energy, the mass plays a crucial role in the investigation of the nuclear structure of radioactive nuclides [1,2]. In particular, the behavior of the two-neutron separation energy S_{2n} along isotopic chains provides information on the general features of the structure of the nuclides as a function of the neutron number N, such as neutron magic numbers, midshell effects, or deformations. As an example, a survey over a large mass region around $Z = 82$ with the ISOLTRAP spectrometer permitted the study of the shape coexistence of even-even neutron-rich isotopes of platinum and mercury, as well as the effect on the binding energy of the mixing of the ground state with low-lying intruder states of polonium isotopes [3]. More recently, a mass measurement campaign of neutron-rich nickel, copper, and gallium isotopes has given insights on midshell structure effects for $N = 40$ [4].

In this work the determination of the atomic masses of neutron-rich krypton isotopes is presented. The measured isotopic chain includes the magic number $N = 50$ and a subshell closure, which is believed to occur at $N = 56$ for $Z \geqslant 36$. No sizable deformation from the spherical shape is expected in the region between $N = 50$ and $N = 58$ [5–7].

The nuclear structure in this region may well have an important effect in astrophysics. The abundance of heavy elements produced by rapid neutron capture (the so-called r process) will be influenced by nuclear effects brought by the binding energy, notably the departure from stabilizing shell or subshell closures [8]. In some scenarios, the r-process path traverses the

region for which new values are reported here. The new mass values are compared to the recent Atomic-Mass Evaluation (AME2003) [9] and the influence on the mass surface with respect to the two-neutron separation energies is discussed.

II. EXPERIMENTAL SETUP AND PROCEDURE

For two decades, ISOLTRAP (Fig. 1) at ISOLDE, CERN has performed high-precision mass measurements for a variety of exotic nuclides [10,11]. A linear and segmented Paul trap filled with helium buffer gas accumulates and cools the radioactive ions [12]. The ions are ejected in bunches and two successive pulsed drift tubes adjust their kinetic energy for a proper injection into the preparation Penning trap. In the latter, the radioactive ions of interest are mass-selectively further cooled by collisions in helium buffer gas during resonant quadrupolar radiofrequency (rf) excitation of the ion motion [13]. With this technique, a mass resolving power of up to 10^5 can be reached with an excitation of several hundreds of milliseconds [14].

The selected ions are injected into the precision Penning trap where their magnetron motion is excited by a dipolar rf field at the magnetron frequency. This results in an expansion of the radius of the magnetron motion. Then a quadrupolar excitation, whose frequency is scanned over several cycles across the expected cyclotron frequency of the ions, converts the slow and low-energetic magnetron motion into the fast and high-energetic cyclotron motion [15,16]. The ions are finally ejected and a micro-channel-plate (MCP) detector is used for a time-of-flight determination.

If the quadrupolar excitation is in resonance with the cyclotron frequency the ions acquire maximum radial energy by a complete conversion of the magnetron motion into cyclotron motion. During ejection, this radial energy is transformed into axial kinetic energy by passing the magnetic field gradient. Thus, the time of flight is minimized [17]. The shape of the
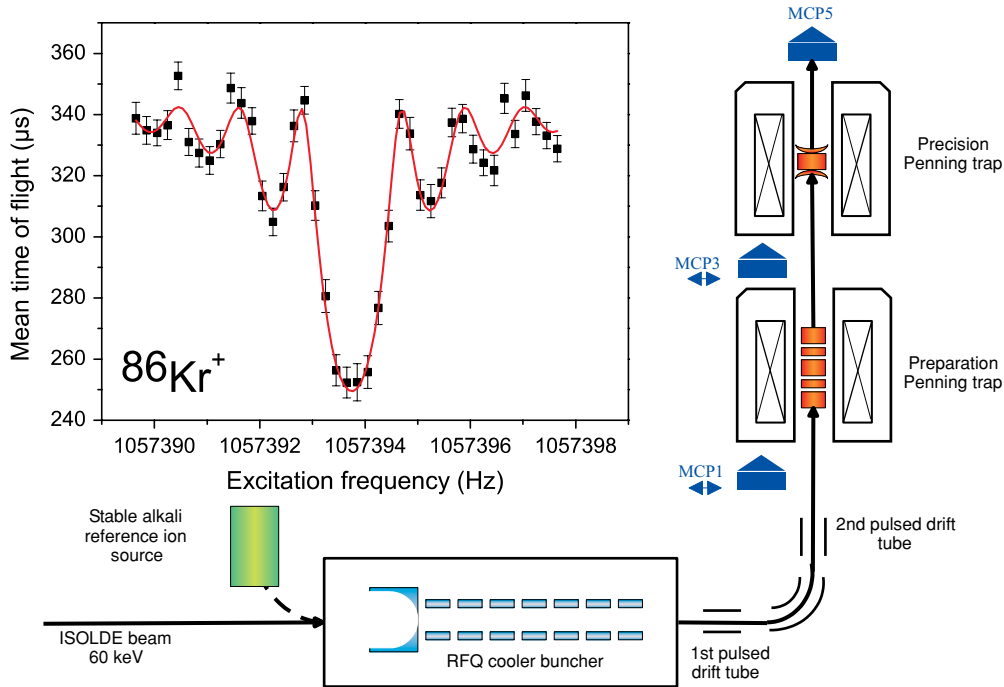

FIG. 1. (Color online) The layout of the tandem Penning trap mass spectrometer ISOLTRAP. Micro-channel-plate detectors (MCP) are used to monitor the ion transfer and to record the time-of-flight resonance. The inset shows a time-of-flight resonance for ^{86}Kr$^+$ with 900 ms excitation duration. The solid line is a fit of the expected line shape to the data points.

time-of-flight cyclotron resonance is well known [16]. As an example, data for ^{86}Kr$^+$ ions along with a fit of the resonance curve is shown in the inset of Fig. 1.

The cyclotron frequency of an ion of mass m and charge q in a magnetic field of magnitude B is given by

$$\nu_c = \frac{1}{2\pi} \cdot \frac{q}{m} \cdot B. \tag{1}$$

The magnetic field is accurately deduced from the determination of the cyclotron frequencies of ions with a well-known mass delivered by the stable alkali reference ion source. The statistical uncertainty associated to the measured cyclotron frequency is empirically related to the number of recorded ions N_{tot} and to the rf excitation time T_{rf} by the following formula:

$$\frac{\sigma_\nu}{\nu_c} = \frac{1}{\nu_c} \frac{c}{\sqrt{N_{tot}} T_{rf}} \tag{2}$$

where σ_ν is the standard deviation of the cyclotron frequency and c a constant that was measured to be $c = 0.898(8)$ for ^{85}Rb [18]. Magnetic field fluctuations and mass-dependent systematic effects also contribute to the total uncertainty. A residual relative mass uncertainty of 8×10^{-9} constitutes the current accuracy limit of ISOLTRAP, as probed by cross-reference measurements with carbon clusters ^{12}C$_n^+$. A detailed discussion of the mass-uncertainty evaluation can be found in Ref. [18].

The neutron-rich krypton was produced in an UC$_x$ target by bombardment with 1.4-GeV proton pulses. The krypton atoms diffused out of the target and effused through a cooled transfer line towards a plasma ion source where they were ionized. An excellent beam purity was achieved by keeping the transfer line at low temperature. The radioactive isotope of interest was then mass-selected by use of the High-Resolution Separator (HRS) of ISOLDE with a resolving power of about 3000 [19]. No isobaric beam contamination was detected. A yield of 1.8×10^8 ions/μC was measured for ^{91}Kr. During the time of the experiment, the proton beam intensity was 1.6×10^{13} protons per pulse (half of the maximum) approximately every 2 s.

For the mass measurement at least two cyclotron resonances were recorded for each isotope. A typical efficiency of 3×10^{-3} for the transmission from the ISOLDE HRS through the spectrometer to the last MCP was estimated for ^{91}Kr. As a reference nuclide, ^{85}Rb from the stable alkali reference ion source was injected into the spectrometer before and after the corresponding krypton isotope cyclotron-frequency measurement. The mass of ^{85}Rb is known with relative uncertainty of 1.6×10^{-10} [20].

III. RESULTS

A summary of the results, in comparison to the AME2003 values, is given in Table I and shown in Fig. 2. Close to the region of stability, the cyclotron frequencies were determined using quadrupolar-excitation durations of 900 ms, reaching a relative uncertainty of a few 10^{-8} for the frequency ratios, i.e., an uncertainty of a few keV for the atomic masses. For the two shortest-lived isotopes ^{94,95}Kr, excitation durations ranging from 100 to 400 ms were applied and a lower number of ions was accumulated, due to the reduced production yield of only a few 100 ions/s. Thus the uncertainty obtained is

TABLE I. Results of the reported mass measurements. r is the ratio of the cyclotron frequency determined for ^{85}Rb$^+$ to the frequency determined for the krypton or rubidium ions. The mass excess of ^{85}Rb is $-82167.331(11)$ keV as measured in Ref. [20]. In the AME2003 [9], the mass values of the ^{94,95}Kr nuclides are estimated from systematic trends and are therefore marked with the symbol #.

Isotope	Half-life $T_{1/2}$	Frequency ratio r	Mass excess ISOLTRAP (keV)	Mass excess AME 2003 (keV)
^{84}Kr	stable	0.9882195709(173)	$-82438.3(1.4)$	$-82431.0(2.8)$
^{86}Kr	stable	1.0117631345(183)	$-83264.3(1.4)$	$-83265.57(10)$
^{87}Kr	76.3 min	1.0235724499(344)	$-80708.6(2.7)$	$-80709.43(27)$
^{87}Rb	stable	1.0235232692(322)	$-84598.5(2.5)$	$-84597.795(12)$
^{88}Kr	2.84 h	1.0353623157(324)	$-79691.3(2.6)$	$-79692(13)$
^{89}Kr	3.15 min	1.0471792153(273)	$-76535.8(2.2)$	$-76730(50)$
^{90}Kr	32.32 s	1.0589761517(232)	$-74959.2(1.8)$	$-74970(19)$
^{91}Kr	8.57 s	1.0708035419(284)	$-70973.9(2.3)$	$-71310(60)$
^{92}Kr	1.840 s	1.0826084190(342)	$-68769.3(2.7)$	$-68785(12)$
^{93}Kr	1.286 s	1.0944440025(312)	$-64136.0(2.5)$	$-64020(100)$
^{94}Kr	210 ms	1.106256253(152)	$-61348(12)$	$-61140(300)$#
^{95}Kr	114 ms	1.118098870(239)	$-56159(19)$	$-56040(400)$#

about one order of magnitude larger for ^{94,95}Kr than for the other isotopes investigated. Figure 3 shows one of the two resonances obtained for ^{95}Kr, with an excitation time of 200 ms and a total of 1618 ions accumulated and detected during about 1 h.

In most of the cases the masses determined from these measurements are in agreement with the AME2003. However, as is clearly visible in Fig. 2, our result for ^{84}Kr deviates by 3σ, and those for ^{89}Kr and ^{91}Kr disagree by 4σ and 6σ, respectively.

The mass of ^{87}Rb, available from the reference ion source, and those of the isotopes ^{86}Kr and ^{87}Kr are better known than currently measurable with ISOLTRAP. In principle they can be used as further reference masses. In the present analysis

they were treated as unknown masses, thus permitting a self-consistency check of the accuracy of the measurements. In all cases, the agreement of the ISOLTRAP results with the AME2003 values is excellent, giving a strong confidence in the measurements of the atomic masses of the exotic nuclides. The data analysis was performed according to the procedure described in Ref. [18]. The uncertainties given in Table I include the statistical as well as the systematic uncertainties.

IV. DISCUSSION OF THE MEASURED MASSES

A. The mass of the stable isotope ^{84}Kr

The AME2003 mass value of ^{84}Kr combines data from four sources, as summarized in Table II. Also given is their respective influence on the mean value as defined in Table II of Ref. [9]. The first value is deduced from a (n, γ) measurement that makes a strong link between the mass of ^{84}Kr and the mass of ^{83}Kr. The second one is a direct measurement of ^{84}Kr
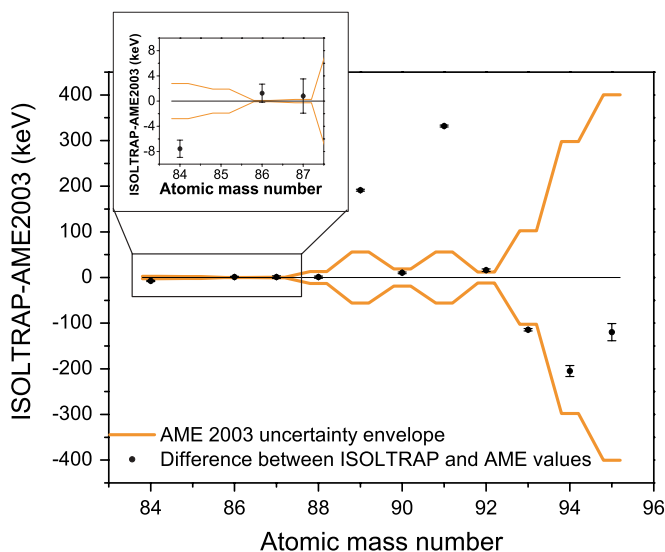

FIG. 2. (Color online) Comparison of the results of the ISOLTRAP mass measurements with the literature values taken from the AME2003 database [9]. The AME2003 mass values of the ^{94,95}Kr nuclides are estimated from systematic trends.
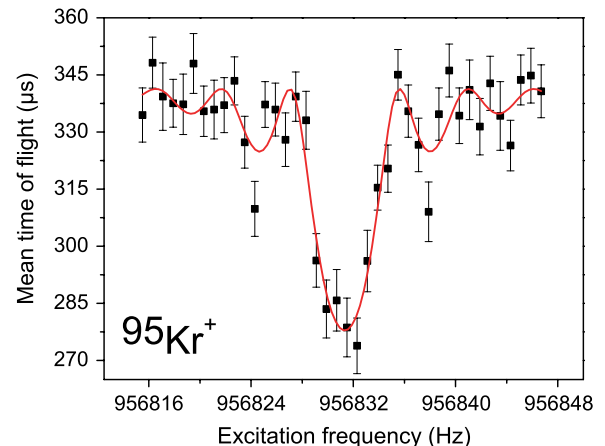

FIG. 3. (Color online) An example of experimental time-of-flight resonance and associated fit, obtained for ^{95}Kr. See text for details.

TABLE II. The sources for the mass of ^{84}Kr as used in AME 2003. The influence of the individual measurements on the AME2003 value is indicated, except in the case of the $Q_{\beta+}$ measurements for which a total influence is given.

Method	Influence (%)	Ref.	Deviation from AME2003 (keV)
^{83}Kr$(n, \gamma)^{84}$Kr	25.1	[21]	0.0(0.3)
C$_6$H$_{12}$ − ^{84}Kr	23.2	[22]	−5.4(6.3)
^{84}Rb$(\beta^+)^{84}$Kr	39.9	[23]	2.0(3.0)
^{84}Rb$(\beta^+)^{84}$Kr		[24]	−1.0(5.0)
^{84}Kr$(d, p)^{85}$Kr	11.8	[25]	−1.0(8.0)
^{84}Kr-^{85}Rb	—	This work	−7.3(1.4)

with respect to C$_6$H$_{12}$, in good agreement with the present result but with a larger uncertainty. The third is a group of two $Q_{\beta+}$ measurements. Finally, a (d, p) measurement, which has a small influence factor, is also in agreement with the present measurement. The deviations of the input values of these measurements from the AME2003 mass value are shown in Fig. 4(a). Two more recent measurements performed at Florida State University with an uncertainty of 6×10^{-11} [26] and at Michigan State University [27] with Penning trap spectrometers are also included. Both are in excellent agreement with our result.

The strong (n, γ) link mainly constrains the mass of ^{83}Kr, with an influence factor of 74.7%, as reported in the AME2003. This explains its relatively small contribution to the mass evaluation of ^{84}Kr with respect to its accuracy. Consequently,
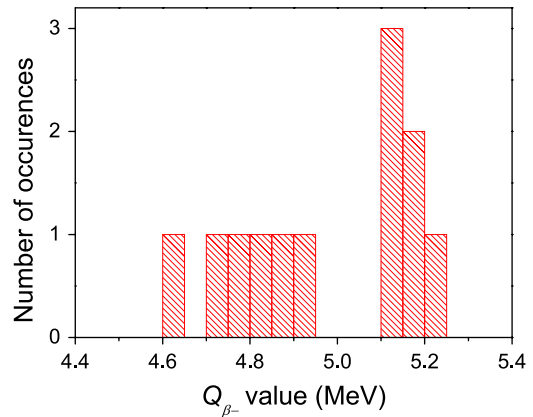

FIG. 5. (Color online) Distribution of the $Q_{\beta-}$ values for the decay of ^{89}Br as in Table 3a of Ref. [29].

the mass of ^{83}Kr as evaluated in Ref. [9] is not correct. In the work presented in Ref. [27], it has been directly measured and its new value is now consistent with the (n, γ) measurement and the latest ^{84}Kr mass values. Thus, the only measurement that does not agree with the ISOLTRAP mass value is the $Q_{\beta+}$ determination presented in Ref. [23]. This latter result was removed in a revised evaluation of the ^{83,84}Kr masses from the Atomic Mass Data Center (AMDC). Using the measurements shown in Fig. 4(b) a mass excess of −82439.297(5) keV has been deduced for ^{84}Kr. The (n, γ) measurement now only constrains the mass of ^{83}Kr and is therefore not shown in this graph.

B. The masses of the radioactive isotopes ^{89,91}Kr

The AME2003 mass values of the ^{89,91}Kr isotopes arise from $Q_{\beta-}$ measurements performed in the 1970s at the TRISTAN on-line separator [28], in the 1980s at the OSIRIS on-line separator [29], and at ISOLDE [30]. No obvious reason for an erroneous Q-value determination was found in the data presented in Refs. [28] and [30] for ^{89,91}Kr; however, a possible mistake was discovered in Ref. [29] for ^{89}Kr. For the latter a distribution of the $Q_{\beta-}$ values for the decay of ^{89}Br, given in Table 3a of Ref. [29], is shown in Fig. 5. A separation into two groups is clearly visible. This indicates that a γ ray could have been missed in the decay spectrum of ^{89}Kr [31]. As a consequence, the spin assignment of the ground state of ^{89}Kr might be erroneous as well and would need to be verified. A new $Q_{\beta-}$ can be calculated for the second (higher energy) group only with a value of 5.14(12) MeV, which would place it in agreement with the present ISOLTRAP result.

C. Other krypton masses

The remaining new mass values are in agreement with the AME2003. Apart from the cases ^{86,87}Kr, which were better known mostly from precise direct [32] and (n,γ) [21] measurements, the uncertainties have been significantly reduced. The corresponding mass values mainly arose from $Q_{\beta-}$ determination and from the well-established masses of the

(a) AME2003 mass evaluation and new measurements
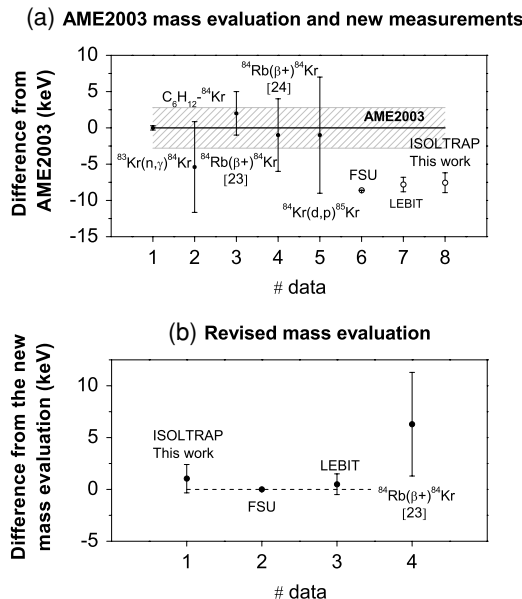
(b) Revised mass evaluation

FIG. 4. (a) Comparison of the results of the latest ^{84}Kr Penning trap mass measurements (open symbols) with the previous measurements (full symbols) used in the AME2003 [9]. The gray area corresponds to the AME2003 uncertainty. (b) Comparison of the results of the measurements used in the revised evaluation of the mass of ^{84}Kr from the AMDC. The line corresponds to the new mass evaluation. For further explanation see text.
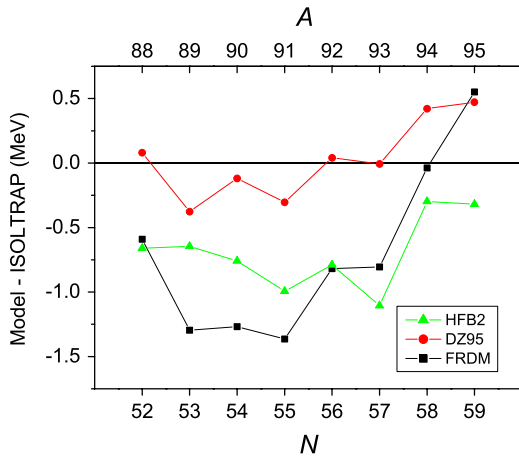
FIG. 6. (Color online) Comparison of the masses of krypton isotopes predicted by the models FRDM [34], DZ95 [35], and HFB2 [36] with the reported measurements as a function of the neutron number N. See text for more details.

rubidium daughter nuclides [9]. Additionally a (t, p) reaction was used in the evaluation of the mass of ^{88}Kr.

D. New krypton masses

As the masses of ^{94,95}Kr were measured for the first time, it is interesting to compare them to mass model predictions that are necessary for the study of stellar nucleosynthesis. Modeling the r process requires mass values of essentially all neutron-rich nuclides to the drip line (see, for example, Ref. [33]). Many mass models based on different approaches have been developed over the years with varying success. A review and comparison was given by Lunney, Pearson, and Thibault [1]. In that work, three models were singled out for their complementary approaches with the hope that at least two

of them might give concordant predictions for the drip line. Those models were the finite range droplet model (FRDM) of Möller *et al.* [34], the shell-model-Hamiltonian-based Duflo-Zuker model [35] and the Skyrme–Hartree-Fock–Bogoliubov model (HFB2) of Goriely *et al.* [36].

Figure 6 shows the predictions of these three models with respect to the new experimental data of this work. The DZ95 model does a significantly better job than the others in reproducing the known data (given the changes reported in this article) and a good job extrapolating to the new values for ^{94,95}Kr. The HFB2 and FRDM model predictions are of more modest quality. Although the FRDM prediction for ^{94}Kr would seem to be perfect, it is most probably fortuitous because neither the lighter (known) data nor the heavier ^{95}Kr data are particularly well accounted for. Indeed, the diverging prediction trend for the FRDM is worrying, whereas the HFB2 model calculations are quite stable. We should bear in mind, however, that this is just one isotopic chain.

Calculating the root-mean-square deviation with respect to the new data of this work for $N = 52$ to $N = 59$ we obtain for FRDM: 944 keV; DZ95: 286 keV; HFB2: 746 keV. These numbers can be compared to the fits obtained for the entire AME2003 mass table [37]: 659, 360, and 656 keV, respectively.

E. Application of the mass values

The present results are relevant for an investigation of the mass surface along the isotopic chain. Some changes are expected because at least 3 of 11 measured mass values are significantly different from the AME2003. The two-neutron separation energies for the neutron-rich krypton and neighboring nuclides from the AME2003 and from the present results are shown in Fig. 7. Recently, masses of neutron-rich Sr, Zr, and Mo isotopes for $N \geqslant 57$ were measured at
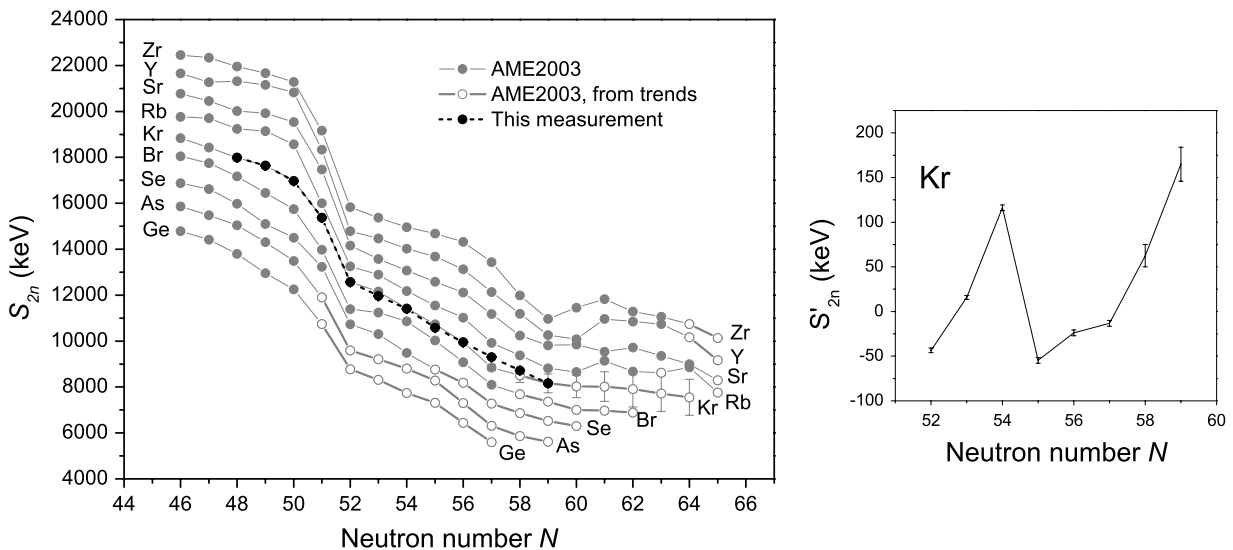

FIG. 7. Two-neutron separation energies as a function of the neutron number for krypton and neighboring elements. The values deduced from the new measurements reported here are shown in dashed lines. (Right) The reduced two-neutron separation energies of the Krypton isotopes as deduced from the ISOLTRAP measurements. For further explanation see text.

the JYFL laboratory [38], confirming the known change of structure between $N = 58$ and $N = 60$ [39].

The general behavior of $S_{2n}(N)$ around the $N = 50$ shell closure is conserved. However, the steeper slope that appears immediately above $N = 56$ for the neighboring isotopes has vanished for krypton. $N = 56$ is commonly quoted in the literature as the $2d_{5/2}$ spherical subshell closure for the heavier elements, with $38 \geqslant Z \geqslant 48$ [40]. Above $N = 52$ and below $N = 59$ the trend is now linear and without any irregularities. A deeper inspection of the mass surface can be made by subtracting the linear trend from the $S_{2n}(N)$ of the krypton isotopes in the region $52 \leqslant N \leqslant 59$. The deduced values, i.e., the reduced two-neutron separation energies $S'_{2n}(N)$, are shown in the right inset of Fig. 7. The subtracted trend has been obtained by a weighted linear fit of the $S_{2n}(N)$ over the whole region of interest. The shape of the $S'_{2n}(N)$ does not exhibit a strong kink at $N = 56$ as it would have been expected in the case of a strong closure. Mainly fluctuations around the statistical average value $S'_{2n}(N) = 0$ can be observed in this area, indicating again a very linear decrease of the $S_{2n}(N)$. These results are consistent with a smooth filling of the $2d_{5/2}$ neutron subshell without big structure change, in favor of Ref. [6], which concludes on nondeformed spherical nuclides below $N = 58$, and in slight contrast with Ref. [41], which predicts a sizable gradual increase of the quadrupole deformation above $N = 50$. They additionally show a quenching of the $N = 56$ gap for $Z = 36$, in contrast with what is suggested in Ref. [7].

Abundance calculations of the rapid neutron-capture (r-process) nucleosynthesis require an enormous amount of nuclear data, not only in terms of the number of nuclides but various nuclear properties. After neutron-capture cross sections, nuclear masses play the most important role because the path of the r process will be determined by the competing (γ, n) dissociation that strongly depends on the neutron-separation energy. Also, the β-decay half-life is determined by the energy available, i.e., the Q_{β^-} value from the mass difference of a given nuclide and its daughter.

Two possible r-process paths are shown in Fig. 8. They have been calculated using the canonical model of Seeger *et al.* [33], with the assumption of constant temperature and neutron flux during a fixed time interval, and (n, γ)-(γ, n) equilibrium, the so-called "waiting-point" concept. ^{95}Kr is seen to lie between the two shell closures at $N = 50$ and $N = 82$ where the waiting points form a bottleneck, leading to the observed abundance peaks. The nuclear input required are the neutron separation energies and Q_{β^-} values, here taken from the mass table of Duflo and Zuker [35], which gives the best mass fit (see Fig. 6), and the β-decay rates, taken from the revised gross theory of Tachibana *et al.* [42]. The neutron-capture time for both paths was 1 s. The temperature and neutron flux values for the two paths are determined from the definition and detailed analysis of the waiting-point approximation validity boundaries by Goriely and Arnould [43].

Finally, a previous measurement performed at the Experimental Storage Ring (ESR) of the GSI facility using the Schottky mass measurement method [44] is lacking calibrants in the range $30 \leqslant Z \leqslant 85$. The new measurements, which have reduced the uncertainty of the neutron-rich Kr mass values for 9 of the 11 isotopes measured, and for 6 far away from
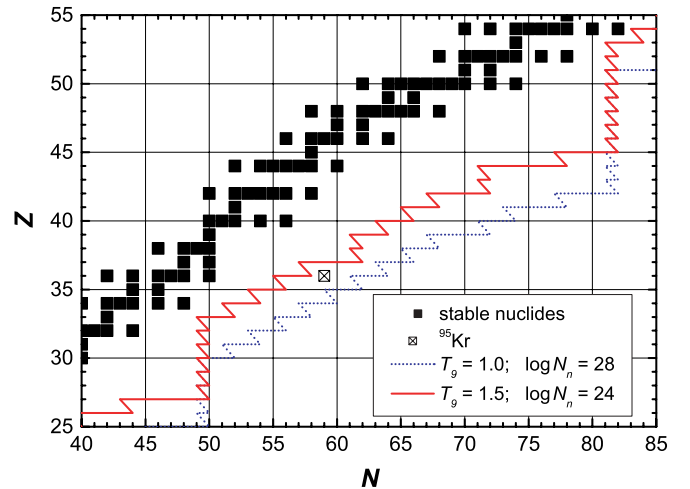

FIG. 8. (Color online) The nuclear chart around $A = 70$–130 with stable nuclides shown as black squares. The nucleus ^{95}Kr is marked by ⊠. Also shown are two possible paths for a rapid neutron-capture process. The temperatures T_9 are expressed in 10^9 K, the neutron density N_n unit is cm^{-3}. For further explanation see text.

stability by at least one order of magnitude, should help to refine the impressive region of the mass surface mapped in that experiment.

V. CONCLUSION AND OUTLOOK

The masses of 11 neutron-rich stable, ^{84,86}Kr, and short-lived, $^{87-95}$Kr, krypton isotopes have been determined with the ISOLTRAP Penning trap mass spectrometer. A significant deviation from the literature value was found for ^{89}Kr and ^{91}Kr. The masses of ^{94}Kr and ^{95}Kr have been measured for the first time.

A quenching of the $N = 56$ spherical subshell gap for $Z = 36$ was observed by scrutinizing the $S_{2n}(N)$ along the measured krypton isotopic chain. Between $N = 52$ and $N = 59$, the linear trend shows a regular filling of the neutron $2d_{5/2}$ and then of the $1g_{7/2}$ subshells, sign of the absence of big structure change in this region.

The vicinity of the astrophysical r-process path, on which ^{96}Kr was recently considered as a possible waiting point [5], has been reached. The predictions of three global mass models were compared to the newly determined masses. The DZ95 model showed quite good agreement, whereas the FRDM and HFB-2 models were less successful. The models also extrapolate quite differently.

Time constraints due to the ISOLDE scheduling rather than any obvious technical limitations at the ISOLTRAP spectrometer prevented the mass measurements of the krypton isotopes further away from stability. It has been recently shown that short-lived isotopes such as ^{32}Ar [45] and ^{74}Rb [46] with half-lives below 100 ms are accessible. According to the yields and lifetimes reported in Ref. [5] mass measurements of $^{96-98}$Kr are possible.

[1] D. Lunney, J. M. Pearson, and C. Thibault, Rev. Mod. Phys. **75**, 1021 (2003).

[2] K. Blaum, Phys. Rep. **425**, 1 (2006).

[3] S. Schwarz *et al.*, Nucl. Phys. **A693**, 533 (2001).

[4] C. Guénaut *et al.*, Eur. Phys. J. A **25**, s01, 33 (2005), and in preparation.

[5] U. C. Bergmann *et al.*, Nucl. Phys. **A714**, 21 (2003).

[6] T. Rzaca-Urban *et al.*, Eur. Phys. J. A **9**, 165 (2000).

[7] G. Lhersonneau, A. Wöhr, B. Pfeiffer, K.-L. Kratz (ISOLDE Collaboration), Phys. Rev. C **63**, 034316 (2001).

[8] J. J. Cowan and F.-K. Thielemann, Physics Today, October 2004, pp. 47–53.

[9] G. Audi, A. H. Wapstra, and C. Thibault, Nucl. Phys. **A729**, 337 (2003).

[10] K. Blaum *et al.*, Nucl. Phys. **A752**, 317 (2005).

[11] F. Herfurth *et al.*, J. Phys. B **36**, 931 (2003).

[12] F. Herfurth *et al.*, Nucl. Instrum. Methods A **469**, 254 (2001).

[13] G. Savard, St. Becker, G. Bollen, H.-J. Kluge, R. B. Moore, Th. Otto, L. Schweikhard, H. Stolzenberg, and U. Wiess, Phys. Lett. **A158**, 247 (1991).

[14] H. Raimbault-Hartmann, D. Beck, G. Bollen, M. König, H.-J. Kluge, E. Schark, J. Stein, S. Schwarz, and J. Szerypo, Nucl. Instrum. Methods B **126**, 378 (1997).

[15] G. Bollen, R. B. Moore, G. Savard, and H. Stolzenberg, J. Appl. Phys. **68**, 4355 (1990).

[16] M. König, G. Bollen, H. -J Kluge, T. Otto, and J. Szerypo, Int. J. Mass Spectrom. Ion Processes **142**, 95 (1995).

[17] G. Gräff, H. Kalinowsky, and J. Traut, Z. Phys. A **297**, 35 (1980).

[18] A. Kellerbauer, K. Blaum, G. Bollen, F. Herfurth, H.-J. Kluge, M. Kuckein, E. Sauvan, C. Scheidenberger, and L. Schweikhard, Eur. Phys. J. D **22**, 53 (2003).

[19] E. Kugler, Hyp. Int. **129**, 23 (2000).

[20] M. P. Bradley, J. V. Porto, S. Rainville, J. K. Thompson, and D. E. Pritchard, Phys. Rev. Lett. **83**, 4510 (1999).

[21] Cited as R. B. Firestone *et al.*, to be published, in Ref. [9].

[22] R. R. Ries, R. A. Damerow, and W. H. Johnson Jr., Phys. Rev. **132**, 1662 (1963).

[23] L. M. Langer, E. H. Spejewski, and D. E. Wortman, Phys. Rev. **133**, B1145 (1964).

[24] H. M. W. Booij, E. A. Van Hoek, H. Van der Molen, W. F. Slot, and J. Blok, Nucl. Phys. **A160**, 337 (1971).

[25] A. M. Hoogenboom, in Ref. [9] (Cited as private communication).

[26] W. Shi, M. Redshaw, and E. G. Myers, Phys. Rev. A **72**, 022510 (2005).

[27] R. Ringle *et al.*, Int. J. Mass Spectrom. **251**, 300 (2006).

[28] F. K. Wohn and W. L. Talbert Jr., Phys. Rev. C **18**, 2328 (1978).

[29] P. Hoff, K. Aleklett, E. Lund, and G. Rudstam, Z. Phys. A **300**, 289 (1981).

[30] M. Graefenstedt, U. Keyser, F. Münnich, and F. Schreiber, Nucl. Phys. **A491**, 373 (1989).

[31] E. A. Henry, W. L. Talbert Jr., and J. R. McConnel, Phys. Rev. C **7**, 222 (1973).

[32] I. Bergström, C. Carlberg, T. Fritioff, G. Douysset, J. Schönfelder, and R. Schuch, Nucl. Instrum. Methods A **487**, 618 (2002).

[33] P. A. Seeger, W. A. Fowler, and D. D. Clayton, Ap. J. S. **11**, 121 (1965), for a more recent description and associated input data, see also V. Bouquelle, N. Cerf, M. Arnould, T. Tachibana, and S. Goriely, Astron. Astrophys. **305**, 1005 (1996).

[34] P. Möller, J. R. Nix, W. D. Myers, and W. J. Swiatecki, At. Data Nucl. Data Tables **59**, 185 (1995).

[35] J. Duflo and A. P. Zuker, Phys. Rev. C **52**, 23(R) (1995), mass table available at: http://csnwww.in2p3.fr/AMDC/theory/du_zu_28.feb95.

[36] S. Goriely, M. Samyn, P.-H. Heenen, J. M. Pearson, and F. Tondeur, Phys. Rev. C **66**, 024326 (2002).

[37] J. M. Pearson and S. Goriely, Nucl. Phys. A (in press).

[38] U. Hager *et al.*, Phys. Rev. Lett. **96**, 042504 (2006).

[39] W. Urban *et al.*, Nucl. Phys. **A689**, 605 (2001).

[40] T. R. Werner, J. Dobaczewsky, M. W. Guidry, W. Nazarewicz, and J. A. Sheikh, Nucl. Phys. **A578**, 1 (1994).

[41] M. Keim, E. Arnold, W. Borchers, U. Georg, A. Klein, R. Neugart, L. Vermeeren, R. E. Silverans, and P. Lievens, Nucl. Phys. **A586**, 219 (1995).

[42] T. Tachibana, M. Yamada, and Y. Yoshida, Prog. Theor. Phys. **84**, 641 (1990).

[43] S. Goriely and M. Arnould, Astron. Astrophys. **312**, 327 (1996).

[44] Yu. A. Litvinov *et al.*, Nucl. Phys. **A756**, 3 (2005).

[45] K. Blaum, G. Audi, D. Beck, G. Bollen, F. Herfurth, A. Kellerbauer, H.-J. Kluge, E. Sauvan, and S. Schwarz, Phys. Rev. Lett. **91**, 260801 (2003).

[46] A. Kellerbauer *et al.*, Phys. Rev. Lett. **93**, 072502 (2004).